Research in Astron. Astrophys. **2012** Vol. **12** No. **11**, 1563–1575
http://www.raa-journal.org *http://www.iop.org/journals/raa*

***R**esearch in*
***A**stronomy and*
***A**strophysics*

Formation flying in elliptic orbits with the J_2 perturbation *

Xi-Yun Hou, Yu-Hui Zhao and Lin Liu

School of Astronomy and Space Science, Nanjing University, Nanjing 210093, China;
silence@nju.edu.cn
Institute of Space Environment and Astrodynamics, Nanjing University, Nanjing 210093, China

Received 2011 November 18; accepted 2012 April 18

Abstract Relative dynamics between the chief satellite and the deputy ones in formation flying is crucial to maintaining the formation. A good choice of the formation usually requires a lower control frequency or less control energy. For formation flying missions in highly elliptic orbits, the well-known C-W equation is not accurate enough. Instead, Lawden's equation is often used. First, the solution to Lawden's equation with a very simple form is deduced. Then the J_2 perturbation is added. It is found that Lawden's solution is not necessarily valid when the J_2 perturbation is considered. Completely discarding Lawden's solution and borrowing the idea of mean orbit elements, two rules to initialize the formation are proposed. The deviation speed is greatly reduced. Different from previous studies on the J_2 perturbation, except for the relatively simple expression for the semi-major axis, the tedious formulae of the long period terms and the short period terms of other orbital elements are not used. In addition, the deviation speed is further reduced by compensation of the nonlinear effects. Finally, a loose control strategy of the formation is proposed. To test the robustness of this strategy, a third body perturbation is added in numerical simulations.

Key words: celestial mechanics

1 INTRODUCTION

Nowadays, formation flying is a technology often used in space missions (Kapila et al. 2000; Scharf et al. 2003; Alfriend et al. 2010). In these missions, several satellites form a special formation. Usually one of them, called the chief satellite, is used to fix the formation in space, and other satellites called deputy ones are around it. The chief satellite can be a real satellite or just an imaginary one. Formation flying has many advantages such as a longer baseline for observation, as well as improved coverage for communication and surveillance, although it also suffers from other problems such as station-keeping of the formation.

The traditional way to treat the relative motions between the chief satellite and the deputy ones is to use the C-W equation (also known as Hill's equation) (Clohessy & Wiltshire 1960). The frame used by this equation is centered at the chief satellite and rotates with it. The x axis points from the central body to the chief satellite. The z axis is parallel to the chief satellite's angular momentum. The y axis forms a right-hand frame with the x and z axes. This frame is usually called the rotating local vertical/local horizontal (LVLH) frame. The C-W equation assumes a circular orbit for the

* Supported by the National Natural Science Foundation of China.

chief satellite. Its solution is simple and can be used to design various formations. However, there are two disadvantages when using it in practice. First, it is inaccurate for formation flying in highly elliptic orbits. Second, it neglects various perturbations such as the non-spherical gravitation terms of the central body (Alfriend et al. 2000). In order to compensate for these two disadvantages, a lot of work has been done. To list a few, see Melton (2000); Baoyin et al. (2002); Inalhan et al. (2002); Schaub & Alfriend (1999).

By expanding the true anomaly as a literal series of the mean anomaly, time explicit solutions of the relative motion can be obtained (Melton 2000; Baoyin et al. 2002). Due to a problem with convergence, these solutions are inconvenient for applying to highly elliptic orbits. In Lawden (1963); Carter & Humi (1987); Inalhan et al. (2002), this problem was overcome by constructing a closed-form periodic solution, with the true anomaly f replacing the time (or the mean anomaly) as an independent variable. The equation describing the small body's motion in the rotation LVLH frame in elliptic orbits is often called Lawden's equation. In this paper, we call the solution to this equation "Lawden's solution." There are various forms of this solution. In this paper, the solution is expressed in a compact form. It can be directly applied at any point to initialize the flying formation.

However, the formation initialized by Lawden's solution gradually deviates when the J_2 perturbation is introduced into the force model. Of course, maneuvers can be used frequently to keep the formation, but the satellites in this case are forced to move on unnatural trajectories and control energy will be wasted. To reduce the effects of deviation due to the J_2 perturbation, the idea of mean orbit elements is borrowed (Brouwer 1959). We find that Lawden's solution is just a special case ($\Delta a = 0$) and does not need to be valid. We completely discard Lawden's solution and propose two rules to initialize the formation. The improvement is obvious. For the first rule, we have four degrees of freedom when choosing initial flying formations. For the second, we have three. Different from previous works in Schaub & Alfriend (1999), except for the semi-major axis a (whose expression is simple), the formulae of the terms describing the long period and the short period for other orbital elements are not used. In addition, the result is further improved by considering nonlinear effects.

Finally, the formation control problem is considered. There are many papers on this subject. To list a few, please see Alfriend et al. (2010); Bauer et al. (1997); Folta et al. (1992); Kristiansen & Nicklasson (2009); Scharf et al. (2004); Schaub et al. (2000); Tillerson & How (2001); Vadali et al. (2002). In our paper, a loose control strategy is proposed. Numerical simulations with the J_2 perturbation are performed to demonstrate this strategy. To test the robustness of the control strategy, the Moon's perturbation is also added into the force model.

2 LAWDEN'S EQUATION

Satellites around a spherically symmetric body follow

$$\ddot{\bar{\boldsymbol{R}}} = -GM\bar{\boldsymbol{R}}/\bar{R}^3\,, \tag{1}$$

where $\bar{\boldsymbol{R}}$ is the position vector of the satellite in a sidereal frame centered at the center body. The transformation $\bar{\boldsymbol{R}} = C\bar{\boldsymbol{r}}$ transfers the vectors in the sidereal frame to the ones in the synodic frame (the frame rotating with the chief satellite). Denote the orbit elements of the chief satellite as $\sigma = (a, e, i, \Omega, \omega, M)^{\mathrm{T}}$. The transformation matrix is defined as $C = R_z(-\Omega)R_x(-i)R_z(-u)$, where $u = \omega + f$ and f is the true anomaly. The units of mass, length and time are defined as

$$[M] = M, \qquad [L] = a, \qquad [T] = \sqrt{[L]^3/G[M]}\,. \tag{2}$$

The dynamical equations in the synodic frame follow

$$\begin{cases} \ddot{\bar{x}} - 2\dot{f}\dot{\bar{y}} - \dot{f}^2\bar{x} - \ddot{f}\bar{y} = -\bar{x}/\bar{r}^3, \\ \ddot{\bar{y}} + 2\dot{f}\dot{\bar{x}} - \dot{f}^2\bar{y} + \ddot{f}\bar{x} = -\bar{y}/\bar{r}^3, \\ \ddot{\bar{z}} = -\bar{z}/\bar{r}^3\,. \end{cases} \tag{3}$$

Re-scale the coordinates as $(\bar{x}, \bar{y}, \bar{z}) = \bar{r}(x, y, z)$ to obtain the scaled synodic frame. The new length unit $\bar{r} = a(1 - e^2)/(1 + e\cos f)$ is the radius of the chief satellite. Taking the true anomaly f as an independent variable, the equations of motion for the satellites can be simplified as (Szebehely 1967)

$$\begin{cases} x'' - 2y' = -\frac{1}{1+e\cos f}(\frac{x}{r} - x), \\ y'' + 2x' = -\frac{1}{1+e\cos f}(\frac{y}{r} - y), \\ z'' + z = -\frac{1}{1+e\cos f}(\frac{z}{r} - z)\,, \end{cases} \tag{4}$$

where e is the orbital eccentricity of the chief satellite, and $r = \sqrt{x^2 + y^2 + z^2}$. The derivation of the above equation can be found in Szebehely (1967). The primes in the equations are defined as (taking x as an example)

$$x' = dx/df, \qquad x'' = d^2x/df^2\,. \tag{5}$$

Equation (4) can also be deduced from the equation of motion for the elliptic restricted three-body problem (ERTBP) by directly setting the mass parameter $\mu = 0$ (Szebehely 1967; Hou & Liu 2011). In the scaled synodic frame, the chief satellite's orbit is expressed as an equilibrium point $(1, 0, 0, 0, 0, 0)^{\mathrm{T}}$. We can move the origin from the central body to the chief satellite to obtain the scaled rotating LVLH frame and denote the deputy satellite's state vector in this frame as $(\xi, \eta, \zeta, \xi', \eta', \zeta')^{\mathrm{T}}$. Then we have $(x, y, z, x', y', z')^{\mathrm{T}} = (\xi, \eta, \zeta, \xi', \eta', \zeta')^{\mathrm{T}} + (1, 0, 0, 0, 0, 0)^{\mathrm{T}}$. Expanding Equation (4) around the chief satellite $(1, 0, 0, 0, 0, 0)^{\mathrm{T}}$ and retaining only the linear part, we have

$$\begin{cases} \xi'' - 2\eta' = \frac{3\xi}{1+e\cos f}, \\ \eta'' + 2\xi' = 0, \\ \zeta'' + \zeta = 0\,. \end{cases} \tag{6}$$

It is easy to obtain the periodic solution as

$$\begin{cases} \xi = \alpha[\cos\theta_1 + e\cos(\theta_1 - f)/2 + e\cos(\theta_1 + f)/2], \\ \eta = \alpha[-2\sin\theta_1 - e\sin(\theta_1 + f)/2], \\ \zeta = \beta\cos\theta_2\,, \end{cases} \tag{7}$$

where

$$\theta_1 = f + \theta_{10}, \qquad \theta_2 = f + \theta_{20}\,. \tag{8}$$

α and β are constants of integration which can be arbitrarily chosen. They indicate the motion amplitudes in and out of the $\xi - \eta$ plane. θ_{10} and θ_{20} are initial phase angles which can also be arbitrarily chosen. Equation (7) is actually the solution to Lawden's equation (more accurately speaking, the conditionally stable solution). Lawden first obtained his equation in the rotating LVLH frame $(\bar{\xi}, \bar{\eta}, \bar{\zeta}, \dot{\bar{\xi}}, \dot{\bar{\eta}}, \dot{\bar{\zeta}})^{\mathrm{T}}$ (Lawden 1963). Using the true anomaly f as the independent variable, Carter and Humi (Carter & Humi 1987; Carter 1990) were able to construct the analytic solution of Lawden's equation. In this paper, we first transform Lawden's equation from the rotating LVLH frame to the scaled rotating LVLH frame $(\xi, \eta, \zeta, \bar{\xi}, \bar{\eta}, \bar{\zeta})^{\mathrm{T}}$ and then obtain Equation (7). Since we deal with the same equation in different coordinates, Equation (7) should be the same as those in Carter & Humi (1987); Carter (1990) after being transformed back to the rotating LVLH frame.

From the first two equations of Equation (7), it is easy to obtain

$$\begin{cases} \xi' = -\frac{3e\sin f}{(4+e\cos f)(1+e\cos f)}\xi + \frac{2(1+e\cos f)}{4+e\cos f}\eta, \\ \eta' = -\frac{(8+6e\cos f+e^2)}{(4+e\cos f)(1+e\cos f)}\xi - \frac{2e\sin f)}{4+e\cos f}\eta\,. \end{cases} \tag{9}$$

Equation (9) is given in the scaled rotating LVLH frame. Using the following relations

$$\begin{cases} \bar{\xi} = r\xi, \quad \dot{\bar{\xi}} = \dot{r}\xi + r\dot{\xi} = \dot{r}\xi + r\xi' \dot{f}, \\ \bar{\eta} = r\eta, \quad \dot{\bar{\eta}} = \dot{r}\eta + r\dot{\eta} = \dot{r}\eta + r\eta' \dot{f}, \end{cases} \qquad \dot{r} = \frac{ae(1-e^2)\sin f}{(1+e\cos f)^2}\dot{f}\,, \tag{10}$$

it is easy to rewrite Equation (9) in the rotating LVLH frame as

$$\begin{cases} \dot{\bar{\xi}} = [\frac{e\sin f}{4+e\cos f}\bar{\xi} + \frac{2(1+e\cos f)}{4+e\cos f}\bar{\eta}]\dot{f}, \\ \dot{\bar{\eta}} = -[\frac{(8+6e\cos f+e^2)}{(4+e\cos f)(1+e\cos f)}\bar{\xi} + \frac{e\sin f(2-e\cos f)}{(4+e\cos f)(1+e\cos f)}\bar{\eta}]\dot{f}\,, \end{cases} \tag{11}$$

where

$$\dot{f} = df/dt = (1+e\cos f)^2/\sqrt{a^3(1-e^2)^3}\,. \tag{12}$$

Equation (9) or Equation (11) can be directly used to initialize the formation at any point in the orbit.

3 THE J_2 PERTURBATION

The formation initialized by Equation (9) or Equation (11) gradually deviates under the J_2 perturbation. In the following, we will find a way to reduce the rate of deviation.

The elliptic orbits are precessing under the J_2 perturbation. The oscillating orbit elements can be separated into three parts (Liu et al. 2006): the mean orbit $\bar{\sigma}$, the short period terms $\sigma_{\rm s}$ (the terms containing M) and the long period terms $\sigma_{\rm l}$ (the terms containing Ω and ω).

$$\sigma = \bar{\sigma} + \sigma_{\rm s} + \sigma_{\rm l}\,. \tag{13}$$

Usually $\sigma_{\rm s}$ and $\sigma_{\rm l}$ are of the order $O(J_2)$. The mean orbit elements $(\bar{\Omega}, \bar{\omega}, \bar{M})$ are precessing with constant rates $(\dot{\bar{\Omega}}, \dot{\bar{\omega}}, \dot{\bar{M}})$. Up to the first order of J_2, they have the following forms (Liu et al. 2006)

$$\dot{\bar{\Omega}} = -\frac{3}{2}\frac{J_2}{\bar{a}^{7/2}}(1-\bar{e}^2)^{-2}\cos\bar{i}\,, \tag{14}$$

$$\dot{\bar{\omega}} = \frac{3}{2}\frac{J_2}{\bar{a}^{7/2}}(1-\bar{e}^2)^{-2}\Big(2-\frac{5}{2}\sin^2\bar{i}\Big)\,, \tag{15}$$

$$\dot{\bar{M}} = \bar{n} + \frac{3}{2}\frac{J_2}{\bar{a}^{7/2}}(1-\bar{e}^2)^{-3/2}\Big(1-\frac{3}{2}\sin^2\bar{i}\Big)\,, \tag{16}$$

where $\bar{n} = \bar{a}^{-3/2}$ and $\bar{a} = a - a_{\rm l} - a_{\rm s}$. In Equations (14)–(16) and the following equations, the central body's radius is used as the length unit. As a result, the central body's radius will not appear in these equations. Up to the first order in J_2, $a_{\rm l} = 0$ and

$$a_{\rm s} = \frac{3}{2}\frac{J_2}{\bar{a}}\Big\{\frac{2}{3}\Big(1-\frac{3}{2}\sin^2\bar{i}\Big)\Big[\Big(\frac{\bar{a}}{\bar{r}}\Big)^3 - (1-\bar{e}^2)^{-3/2}\Big] + \sin^2\bar{i}\Big(\frac{\bar{a}}{\bar{r}}\Big)^3\cos 2(\bar{f}+\bar{\omega})\Big\}\,. \tag{17}$$

In Equation (17), $\bar{f}$ is the mean value of f. The quantity $\bar{r}$ is defined as $\bar{r} = \bar{a}(1-\bar{e}^2)/(1+\bar{e}\cos\bar{f})$, different from the definition in Equation (3). The orbit elements $(\bar{a}, \bar{e}, \bar{i})$ do not precess under the J_2 perturbation. In Equation (16), expanding

$$\bar{n} = \bar{a}^{-3/2} = (a-a_{\rm s})^{-3/2} \approx a^{-3/2}\Big(1+\frac{3}{2}a_{\rm s}/a\Big),$$

substituting Equation (17) and adding the result to Equation (15), it is easy to obtain

$$\dot{\bar{M}} + \dot{\bar{\omega}} = a^{-3/2} + \frac{3}{2}\frac{J_2}{\bar{a}^{7/2}}\Big(\frac{\bar{a}}{\bar{r}}\Big)^3(1-3\sin^2\bar{\phi}) + \frac{3}{2}\frac{J_2}{\bar{a}^{7/2}}(1-\bar{e}^2)^{-2}\Big(2-\frac{5}{2}\sin^2\bar{i}\Big) + O(J_2^2)\,, \tag{18}$$

where $\sin\bar{\phi} = \sin\bar{i}\sin\bar{u}$. If the oscillating orbit elements σ are substituted into Equation (14) and Equation (18) instead of the mean orbit elements $\bar{\sigma}$, the difference is of the order $O(J_2^2)$ which can be omitted because perturbations from other non-spherical terms and the third bodies are of this order.

If the deviation between the chief satellite and the deputy one is required to be as small as possible, the following two conditions should hold (Schaub & Alfriend 1999)

$$\Delta\dot{\bar{\Omega}} = \dot{\bar{\Omega}}_{\text{deputy}} - \dot{\bar{\Omega}}_{\text{chief}} = 0\,, \tag{19}$$

$$\Delta(\dot{\bar{M}} + \dot{\bar{\omega}}) = (\dot{\bar{M}} + \dot{\bar{\omega}})_{\text{deputy}} - (\dot{\bar{M}} + \dot{\bar{\omega}})_{\text{chief}} = 0\,. \tag{20}$$

To first order, Equation (19) and Equation (20) mean

$$\Delta\dot{\bar{\Omega}} = \frac{\dot{\bar{\Omega}}}{\partial a}\Delta a + \frac{\dot{\bar{\Omega}}}{\partial e}\Delta e + \frac{\dot{\bar{\Omega}}}{\partial i}\Delta i = 0\,, \tag{21}$$

$$\begin{aligned}\Delta(\dot{\bar{M}} + \dot{\bar{\omega}}) = {} & \tfrac{(\dot{\bar{M}}+\dot{\bar{\omega}})}{\partial a}\Delta a + \tfrac{(\dot{\bar{M}}+\dot{\bar{\omega}})}{\partial e}\Delta e + \tfrac{(\dot{\bar{M}}+\dot{\bar{\omega}})}{\partial i}\Delta i \\ & + \tfrac{(\dot{\bar{M}}+\dot{\bar{\omega}})}{\partial(a/r)}\Delta\tfrac{a}{r} + \tfrac{(\dot{\bar{M}}+\dot{\bar{\omega}})}{\partial(\sin\phi)}\Delta(\sin\phi) = 0\,.\end{aligned} \tag{22}$$

Before proceeding, the state vectors in different frames in this paper should be clarified. $(\bar{X}, \bar{Y}, \bar{Z}, \dot{\bar{X}}, \dot{\bar{Y}}, \dot{\bar{Z}})^{\mathrm{T}}$ indicates the state vector in the sidereal frame centered at the central body. $(\bar{x}, \bar{y}, \bar{z}, \dot{\bar{x}}, \dot{\bar{y}}, \dot{\bar{z}})^{\mathrm{T}}$ indicates the state vector in the synodic frame centered at the central body. (x, y, z, x', y', z') indicates the state vector in the scaled synodic frame. $(\bar{\xi}, \bar{\eta}, \bar{\zeta}, \dot{\bar{\xi}}, \dot{\bar{\eta}}, \dot{\bar{\zeta}})^{\mathrm{T}}$ indicates the state vector in the rotating LVLH frame. $(\xi, \eta, \zeta, \xi', \eta', \zeta')^{\mathrm{T}}$ indicates the state vector in the scaled rotating LVLH frame. In the following discussions, we mainly use the LVLH frame. We use $(\tilde{\xi}, \tilde{\eta}, \tilde{\zeta}, \tilde{\xi}', \tilde{\eta}', \tilde{\zeta}')^{\mathrm{T}}$ to indicate the state vector in the LVLH frame.

From the geometry of elliptic orbits, it is easy to obtain the following linear relations

$$\Delta a = \frac{2a^2}{r^2}\tilde{\xi} + \frac{2}{n\sqrt{1-e^2}}[e\sin f\dot{\tilde{\xi}} + (1+e\cos f)\dot{\tilde{\eta}}]\,, \tag{23}$$

$$\Delta e = \frac{\cos f + e}{r}\tilde{\xi} + \frac{\sin f}{a}\tilde{\eta} + \frac{\sqrt{1-e^2}}{na}\Big[\sin f\dot{\tilde{\xi}} + \frac{2\cos f + e + e\cos^2 f}{1+e\cos f}\dot{\tilde{\eta}}\Big]\,, \tag{24}$$

$$\Delta i = \frac{\sin u + e\sin\omega}{a(1-e^2)}\tilde{\zeta} + \frac{\sqrt{a(1-e^2)}\cos u}{(1+e\cos f)}\dot{\tilde{\zeta}}\,, \tag{25}$$

$$\Delta\Big(\frac{a}{r}\Big) = \frac{1}{r}\Delta a - \frac{a}{r^2}\tilde{\zeta}\,, \tag{26}$$

$$\Delta(\sin\phi) = \frac{\sin i\cos u}{r}\tilde{\eta} + \frac{\cos i}{r}\tilde{\zeta}\,. \tag{27}$$

Substituting Lawden's solution (more accurately speaking, Lawden's solution of the ξ and η components) into Equation (23), we find $\Delta a = 0$, which is a necessary condition to fulfill the formation flying in the two-body problem. However, this condition ($\Delta a = 0$) is unnecessary when the J_2 perturbation is considered, because the precession rate of $\Delta\Omega$ and $\Delta(M+\omega)$ caused by J_2 can be zero even when $\Delta a \neq 0$. Substituting Equations (23)–(27) into Equation (21) and Equation (22), it is easy to obtain

$$\begin{cases}\Delta(\dot{\bar{\Omega}}) = A_1\tilde{\xi} + A_2\tilde{\eta} + A_3\dot{\tilde{\xi}} + A_4\dot{\tilde{\eta}} + A_5\tilde{\zeta} + A_6\dot{\tilde{\zeta}} = 0\,, \\ \Delta(\dot{\bar{M}} + \dot{\bar{\omega}}) = B_1\tilde{\xi} + B_2\tilde{\eta} + B_3\dot{\tilde{\xi}} + B_4\dot{\tilde{\eta}} + B_5\tilde{\zeta} + B_6\dot{\tilde{\zeta}} = 0\,.\end{cases} \tag{28}$$

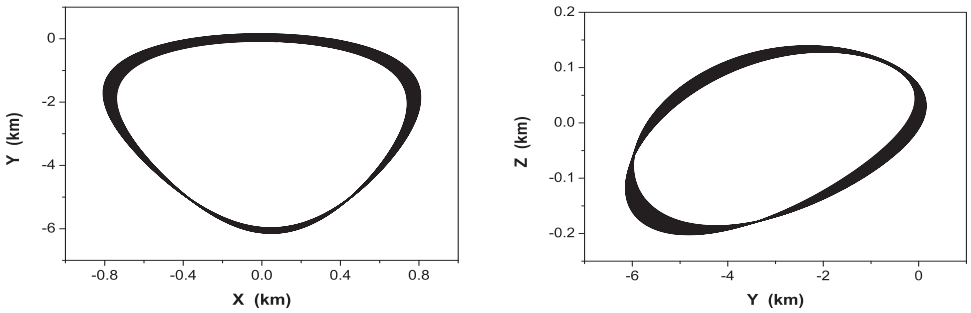

Fig. 1 In-plane formation and out-of-plane formation with the J_2 perturbation for 50 revolutions. The initial formation is given by Eq. (28).

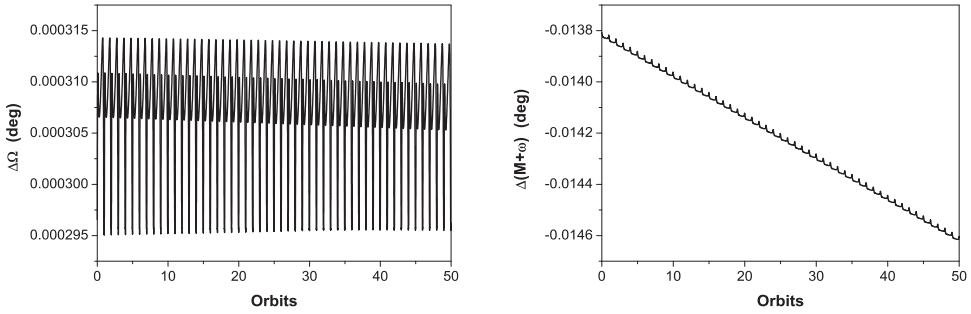

Fig. 2 The history curves of $\Delta\Omega$ and $\Delta(M+\omega)$ of the deputy satellite with respect to the chief satellite, corresponding to Fig. 1.

The coefficients in Equation (28) can be found in the appendix. This is the first rule to initialize the formation. There are four degrees of freedom in selecting the initial formation. In this paper, $\bar{\xi}, \tilde{\eta}, \bar{\zeta}$ and $\dot{\bar{\zeta}}$ can be chosen to have any values and $\dot{\bar{\xi}}$ and $\dot{\tilde{\eta}}$ are then solved from Equation (28).

Figure 1 shows the in-plane formation and the out-of-plane formation using this rule. $J_2 = 1.0820 \times 10^{-3}$. In the following figures, X, Y and Z denote respective variables in the transformed frame. The center body is the Earth. The orbit elements for the chief at the formation initialization point are $a = 1.3156 \times 10^7$ m, $e = 0.5$, $i = 45°$, $\Omega = 0°$, $\omega = 30°$, $f = 30°$. $\bar{\xi} = 344.2817$ m, $\bar{\eta} = 0$ m, $\bar{\zeta} = 68.8564$ m and $\dot{\bar{\zeta}} = 0.1070$ m s^{-1}. The two speeds $\dot{\bar{\xi}} = 0.9664$ m s^{-1} and $\dot{\tilde{\eta}} = -0.4864$ m s^{-1} are computed from Equation (28).

Figure 2 shows the corresponding history curves of $\Delta\Omega$ and $\Delta(M+\omega)$. Judging from Figure 2, it seems that the in-plane deviation rate is larger than that of the out-of-plane deviation. This phenomenon is caused by the nonlinear terms omitted in Equations (21), (22) and (23)–(27). Suppose $\dot{\bar{\xi}}$ and $\dot{\tilde{\eta}}$ are solved from Equation (28) for given $\bar{\xi}, \tilde{\eta}, \bar{\zeta}$ and $\dot{\bar{\zeta}}$, then the chief satellite's oscillating orbital elements (a, e, i) and the deputy satellite's oscillating orbital elements (a', e', i') can be rigorously computed. Substituting them into Equations (14) and (18), we have

$$\begin{cases} \Delta\dot{\bar{\Omega}}_{\text{nonlinear}} = \dot{\bar{\Omega}}_{\text{deputy}} - \dot{\bar{\Omega}}_{\text{chief}}, \\ \Delta(\dot{\bar{M}} + \dot{\bar{\omega}})_{\text{nonlinear}} = (\dot{\bar{M}} + \dot{\bar{\omega}})_{\text{deputy}} - (\dot{\bar{M}} + \dot{\bar{\omega}})_{\text{chief}}. \end{cases} \tag{29}$$

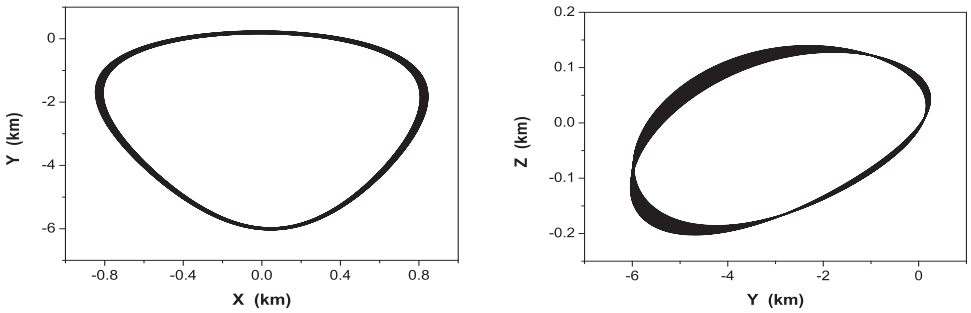

Fig. 3 In-plane formation and out-of-plane formation with the J_2 perturbation for 50 revolutions. The initial formation is firstly given by Eq. (28) and then refined by Eq. (30).

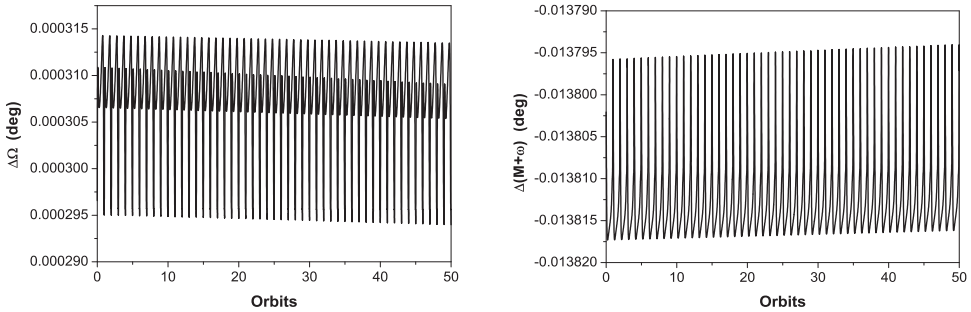

Fig. 4 The history curves of $\Delta\Omega$ and $\Delta(M+\omega)$ of the deputy satellite with respect to the chief satellite, corresponding to Fig. 3.

Since Equation (28) is deduced only using linear relations, $\Delta\dot{\bar{\Omega}}_{\rm nonlinear}$ and $\Delta(\dot{\bar{M}}+\dot{\bar{\omega}})_{\rm nonlinear}$ usually do not equal zero. Computations show that the nonlinear effect of the in-plane motion is larger, which leads to different behaviors in the two frames in Figure 2. If we rewrite Equation (28) as

$$\begin{cases} A_1\tilde{\xi}+A_2\tilde{\eta}+A_3\dot{\tilde{\xi}}+A_4\dot{\tilde{\eta}}+A_5\tilde{\zeta}+A_6\dot{\tilde{\zeta}}+\Delta\dot{\bar{\Omega}}_{\rm nolinear}=0, \\ B_1\tilde{\xi}+B_2\tilde{\eta}+B_3\dot{\tilde{\xi}}+B_4\dot{\tilde{\eta}}+B_5\tilde{\zeta}+B_6\dot{\tilde{\zeta}}+\Delta(\dot{\bar{M}}+\dot{\bar{\omega}})_{\rm nonlinear}=0\,, \end{cases} \tag{30}$$

and solve $\dot{\tilde{\xi}},\dot{\tilde{\eta}}$ again for given $\tilde{\xi},\tilde{\eta},\tilde{\zeta},\dot{\tilde{\zeta}}$, the nonlinear effects can be compensated. For the same initial conditions in Figure 1, the speeds computed by Equation (30) are $\dot{\tilde{\xi}}=0.9660$ m s^{-1} and $\dot{\tilde{\eta}}=-0.4864$ m s^{-1}.

Figure 3 shows the in-plane formation and the out-of-plane formation. Figure 4 shows the corresponding history curves of $\Delta\Omega$ and $\Delta(M+\omega)$. Compared with Figure 2, the in-plane deviation is obviously reduced.

Equation (28) is in fact a way to achieve the so-called J_2 invariant orbit (Schaub & Alfriend 1999), but expressed in the LVLH frame. In addition, Equation (30) is improved with the nonlinear compensation.

The condition $\Delta(\dot{\bar{M}}+\dot{\bar{\omega}})=0$ may cause the case that $\Delta\dot{\bar{M}}$ and $\Delta\dot{\bar{\omega}}$ do not equal zero but their values are opposite in sign. In this case, due to the gradual increase of ΔM, the oscillating amplitude of the formation also gradually increases.

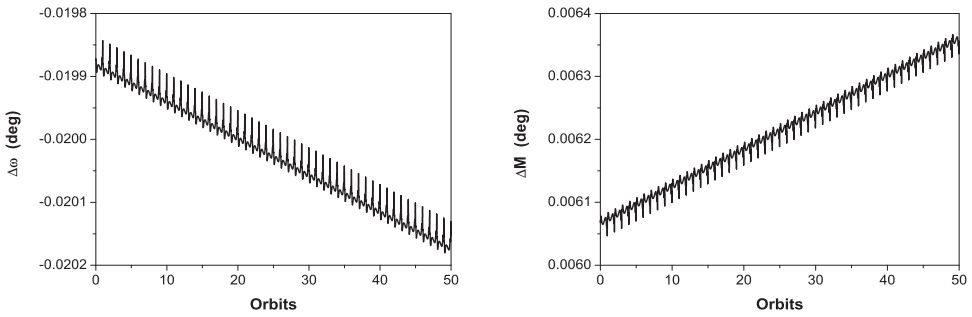

Fig. 5 The history curves of $\Delta\Omega$ and $\Delta(M+\omega)$ of the deputy satellite with respect to the chief satellite, corresponding to Fig. 4.

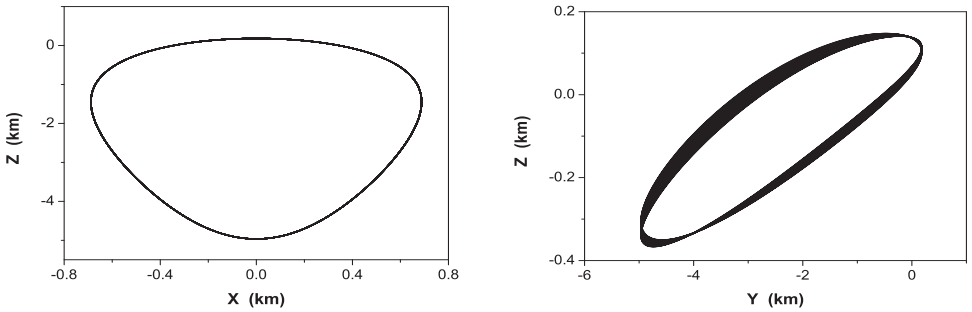

Fig. 6 In-plane formation and out-of-plane formation with the J_2 perturbation for 50 revolutions. The initial formation is firstly given by Eq. (31) and then refined by Eq. (32).

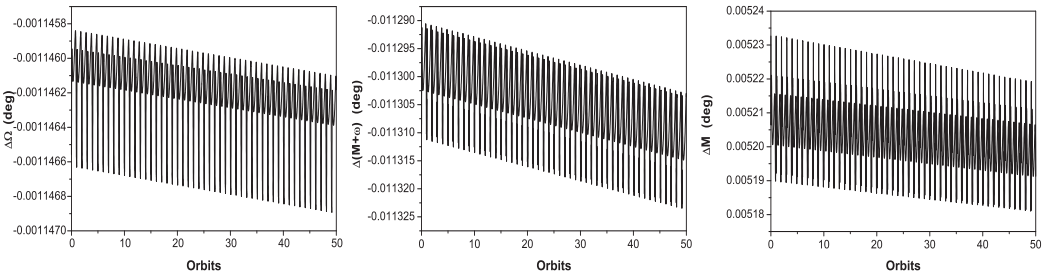

Fig. 7 The history curves of $\Delta\Omega$, $\Delta(M+\omega)$ and ΔM of the deputy satellite with respect to the chief satellite, corresponding to Fig. 6.

Figure 5 shows the history curves of $\Delta\omega$ and ΔM respectively corresponding to those in Figure 4, which demonstrates an example of this phenomenon.

To avoid this situation, we can additionally demand $\Delta\dot{M}=0$. As a result, Equations (28) and (30) are improved as

$$\begin{cases} \Delta(\dot{\Omega}) = A_1\tilde{\xi} + A_2\tilde{\eta} + A_3\dot{\tilde{\xi}} + A_4\dot{\tilde{\eta}} + A_5\tilde{\zeta} + A_6\dot{\tilde{\zeta}} = 0, \\ \Delta(\dot{M}+\dot{\omega}) = B_1\tilde{\xi} + B_2\tilde{\eta} + B_3\dot{\tilde{\xi}} + B_4\dot{\tilde{\eta}} + B_5\tilde{\zeta} + B_6\dot{\tilde{\zeta}} = 0, \\ \Delta\dot{M} = C_1\tilde{\xi} + C_2\tilde{\eta} + C_3\dot{\tilde{\xi}} + C_4\dot{\tilde{\eta}} + C_5\tilde{\zeta} + C_6\dot{\tilde{\zeta}} = 0\,, \end{cases} \tag{31}$$

$$\begin{cases} A_1\tilde{\xi} + A_2\tilde{\eta} + A_3\dot{\tilde{\xi}} + A_4\dot{\tilde{\eta}} + A_5\tilde{\zeta} + A_6\dot{\tilde{\zeta}} + \Delta\dot{\bar{\Omega}}_{\mathrm{nolinear}} = 0, \\ B_1\tilde{\xi} + B_2\tilde{\eta} + B_3\dot{\tilde{\xi}} + B_4\dot{\tilde{\eta}} + B_5\tilde{\zeta} + B_6\dot{\tilde{\zeta}} + \Delta(\dot{\bar{M}} + \dot{\bar{\omega}})_{\mathrm{nonlinear}} = 0, \\ C_1\tilde{\xi} + C_2\tilde{\eta} + C_3\dot{\tilde{\xi}} + C_4\dot{\tilde{\eta}} + C_5\tilde{\zeta} + C_6\dot{\tilde{\zeta}} + \Delta\dot{\bar{M}}_{\mathrm{nonlinear}} = 0\,, \end{cases} \tag{32}$$

where the coefficients A_i and B_i are the same as Equation (28). The coefficients C_i can be found in the appendix.

Figure 6 shows the in and out-of-plane formations initialized by Equations (31) and (32). The initial coordinates are the same as in Figures 1 and 3.

Figure 7 shows the history curves of $\Delta\omega$ and ΔM. Obviously, the deviation speed is greatly reduced by the choice $\Delta\dot{\bar{M}} = 0$. The in-plane formation is also improved by this choice.

4 A LOOSE CONTROL STRATEGY

About the formation control problem, a lot of work has been done. In this paper, however, we propose a loose control strategy which only controls the deputy around the chief, but with no requirements on the exact formation. Due to the nonlinear terms, the deviation between the chief and the deputy still exists, where even the nonlinear effects are partially compensated by Equations (30) and (32). We denote the long term rate of deviation between the chief and the deputy of Ω, $\omega + M$ and M at the control point as Δ_1, Δ_2 and Δ_3 respectively. We can also control the speed to compensate Δ_1, Δ_2 and Δ_3. The maneuvers are then solved from

$$\begin{cases} A_3\Delta\dot{\tilde{\xi}} + A_4\Delta\dot{\tilde{\eta}} + A_6\Delta\dot{\tilde{\zeta}} + \Delta_1 = 0, \\ B_3\Delta\dot{\tilde{\xi}} + B_4\Delta\dot{\tilde{\eta}} + B_6\Delta\dot{\tilde{\zeta}} + \Delta_2 = 0, \\ C_3\Delta\dot{\tilde{\xi}} + C_4\Delta\dot{\tilde{\eta}} + C_6\Delta\dot{\tilde{\zeta}} + \Delta_3 = 0\,, \end{cases} \tag{33}$$

where Δ_1, Δ_2 and Δ_3 can be approximately computed as follows (using Δ_1 as an example). We take

$$\frac{1}{T}\int_0^T \Delta\Omega \cdot dt \tag{34}$$

in one revolution as the approximate value of $\Delta\bar{\Omega}$, where T is the period of one revolution. We denote the value of $\Delta\bar{\Omega}$ in the first revolution and the last revolution before maneuvering respectively as $\Delta\bar{\Omega}_{\mathrm{s}}$ and $\Delta\bar{\Omega}_t$, then

$$\Delta_1 = \frac{\Delta\bar{\Omega}_t - \Delta\bar{\Omega}_{\mathrm{s}}}{NT}\,, \tag{35}$$

where N is the number of revolutions between the first revolution and the last revolution before maneuvering. Of course, these formulae are just approximate, because we ignore the long period terms which may act as long terms in short times. However, our numerical simulations show that this strategy does work.

Figure 8 shows the formation by this loose control strategy. Figure 9 shows the time history of $\Delta\Omega$, $\Delta(\omega + M)$ and ΔM.

Figures 10 and 11 show the results corresponding to no orbit control. The initial conditions are $\bar{\xi} = 6378.1363$ m, $\bar{\eta} = 6378.1363$ m and $\bar{\zeta} = 6378.1363$ m. The speeds $\dot{\bar{\xi}} = 6.1608$ m s^{-1}, $\dot{\bar{\eta}} = -6.9738$ m s^{-1} and $\dot{\bar{\zeta}} = -13.1340$ m s^{-1} are computed from Equation (31) along with Equation (32). The orbit elements for the chief at the initialization point of the formation are $a = 1.3156 \times 10^7$ m, $e = 0.5$, $i = 88^\circ$, $\Omega = 0^\circ$, $\omega = 30^\circ$ and $f = 30^\circ$. Every 1000 revolutions (about 173.2184 days), one orbit control is done. An 869.0935 day (5000 revolution) mission requires energy of only 0.0944 m s^{-1}. In order to test the robustness of the control strategy, the Moon's perturbation is added into the force model. We assume the Moon is in the equatorial plane of the

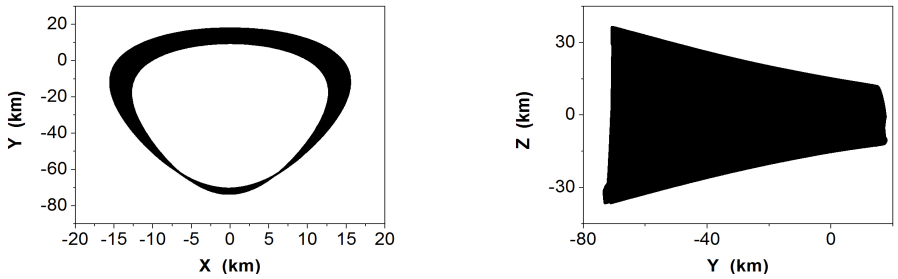

Fig. 8 In-plane formation and out-of-plane formation with the J_2 perturbation for 5000 revolutions with orbit control.

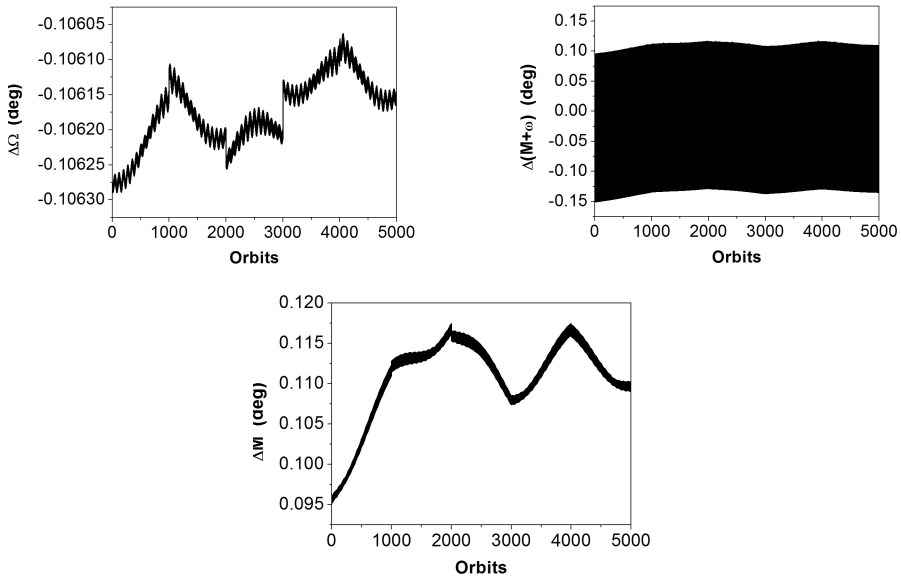

Fig. 9 The history curves of $\Delta\Omega$, $\Delta(M+\omega)$ and ΔM of the deputy satellite with respect to the chief satellite, corresponding to Fig. 8.

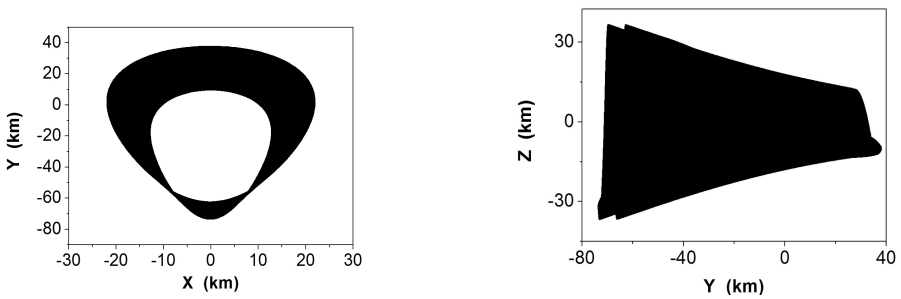

Fig. 10 In-plane formation and out-of-plane formation with the J_2 perturbation for 5000 revolutions without orbit control.

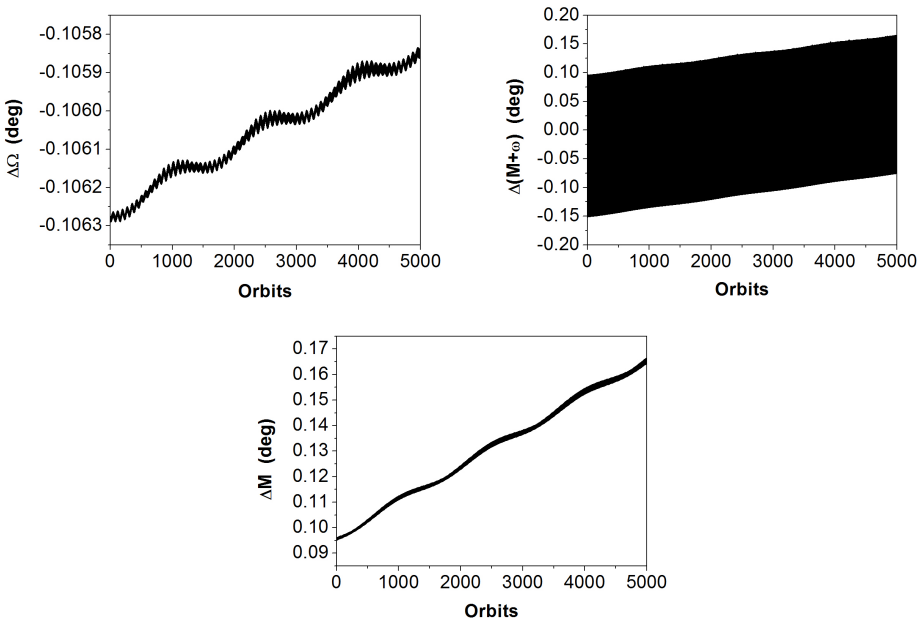

Fig. 11 The history curves of $\Delta\Omega$, $\Delta(M+\omega)$ and ΔM of the deputy satellite with respect to the chief satellite, corresponding to Fig. 10.

Earth and moves with a circular orbit. The semi-major axis of the Moon's orbit is 3.8400×10^5 km. The initial position of the Moon is on the x axis. This simulation is performed to test the robustness of the control algorithm under perturbations, but does not intend to simulate the real situations in which other perturbations besides that of the Moon exist. So the Moon is simply placed in the equatorial plane. If the Moon is placed in a different plane or at a different initial position, different results will be expected.

5 CONCLUSIONS

This paper studied the relative dynamics of formation flying. First, a compact form to Lawden's solution was obtained. However, this solution gradually deviates under the J_2 perturbation. Borrowing the idea of mean orbit elements, two rules of formation initialization were proposed to reduce the rate of deviation. A loose control strategy was also proposed. Numerical simulations were done to demonstrate and test the robustness of this strategy.

Acknowledgements This work was supported by the National Natural Science Foundation of China (Grant Nos. 10903002, 11078001, 11033099 and 11003009).

Appendix A:

$$A_1 = \frac{J_2 \cos i}{a^{9/2}(1-e^2)^4}\left(\frac{15}{2} + 15e\cos f + \frac{9}{2}e^2\cos^2 f - 6e^2 - 6e^3\cos f\right), \tag{A.1}$$

$$A_2 = -\frac{6J_2 e\cos i}{a^{9/2}(1-e^2)^3}\sin f, \qquad A_3 = -\frac{9J_2 e\cos i}{2a^3(1-e^2)^{5/2}}\sin f, \tag{A.2}$$

$$A_4 = \frac{J_2\cos i}{2a^3(1-e^2)^{5/2}}\frac{21+18e\cos f-12e^2+9e^2\cos^2 f}{(1+e\cos f)}, \tag{A.3}$$

$$A_5 = -\frac{3J_2 e\sin i}{2a^{9/2}(1-e^2)^3}(\sin u + e\sin\omega), \qquad A_6 = \frac{3J_2\sin i}{2a^3(1-e^2)^{3/2}}\frac{\cos u}{(1+e\cos f)}, \tag{A.4}$$

$$\begin{aligned} B_1 = {} & -\frac{3(e\cos f)^2}{a^{5/2}(1-e^2)^2} - \frac{3J_2}{2a^{9/2}}\left(\frac{a}{r}\right)^4(1-3\sin^2\phi)\left(\frac{a}{r}+3\right) \\ & -\frac{J_2}{a^{9/2}(1-e^2)^3}\left(\frac{21}{2}+\frac{9}{2}e\cos f-6e^2\right)\left(2-\frac{5}{2}\sin^2 i\right)\left(\frac{a}{r}\right), \end{aligned} \tag{A.5}$$

$$B_2 = -\frac{9J_2}{2a^{9/2}}\left(\frac{a}{r}\right)^4\sin^2\phi + \frac{6J_2}{a^{9/2}(1-e^2)^3}\left(2-\frac{5}{2}\sin f\right), \tag{A.6}$$

$$\begin{aligned} B_3 = {} & -\frac{3e\sin f}{a\sqrt{1-e^2}} - \frac{3J_2}{2a^3(1-e^2)^{3/2}}\left(\frac{a}{r}\right)^2(1-3\sin^2\phi)e\sin f(1+e\cos f) \\ & -\frac{9J_2 e}{2a^3(1-e^2)^{5/2}}\left(2-\frac{5}{2}\sin^2 i\right)\sin f, \end{aligned} \tag{A.7}$$

$$\begin{aligned} B_4 = {} & -\frac{3(1+e\cos f)}{a\sqrt{1-e^2}} - \frac{3J_2}{2a^3(1-e^2)^{3/2}}\left(\frac{a}{r}\right)^2(1-3\sin^2\phi)(1+e\cos f)^2 \\ & -\frac{J_2(2-5/2\sin^2 i)}{2a^3(1-e^2)^{5/2}(1+e\cos f)}\frac{21+18e\cos f-12e^2+9e^2\cos^2 f}{1+e\cos f}, \end{aligned} \tag{A.8}$$

$$B_5 = -\frac{9J_2}{a^{9/2}}\left(\frac{a}{r}\right)^4\cos i\sin\phi - \frac{15J_2\sin i\cos i}{2a^{9/2}(1-e^2)^3}(\sin u + e\sin\omega), \tag{A.9}$$

$$B_6 = -\frac{15J_2\sin i\cos i}{2a^3(1-e^2)^{3/2}(1+e\cos f)}\cos u, \tag{A.10}$$

$$C_1 = -\frac{3}{a^{5/2}}\left(\frac{a}{r}\right)^2 - \frac{3J_2}{2a^{9/2}}\left(\frac{a}{r}\right)^5(1-3\sin^2\phi) - \frac{9J_2}{2a^{9/2}}\left(\frac{a}{r}\right)^4(1-3\sin^2\phi), \tag{A.11}$$

$$C_2 = -\frac{9J_2}{a^{9/2}}\left(\frac{a}{r}\right)^4\sin\phi\sin i\cos u, \tag{A.12}$$

$$C_3 = -\left[\frac{3}{a^{5/2}} + \frac{3J_2}{2a^{9/2}}\left(\frac{a}{r}\right)^3(1-3\sin^2\phi)\right]\frac{e\sin f}{\sqrt{a^3(1-e^2)}}, \tag{A.13}$$

$$C_4 = -\left[\frac{3}{a^{5/2}} + \frac{3J_2}{2a^{9/2}}\left(\frac{a}{r}\right)^3(1-3\sin^2\phi)\right]\frac{1+e\cos f}{\sqrt{a^3(1-e^2)}}, \tag{A.14}$$

$$C_5 = -\frac{9J_2}{a^{9/2}}\left(\frac{a}{r}\right)^4\sin\phi\cos i, \tag{A.15}$$

$$C_6 = 0. \tag{A.16}$$

References

Alfriend, K. T., Schaub, H., & Gim, D. W. 2000, Advances in the Astronautical Sciences, 104, 139
Alfriend, K. T., Breger, L. S., Gurfil, P., Vadali, S. R., & How, J. P. 2010, Spacecraft Formation Flying: Dynamics, Control, and Navigation (Oxford: Elsevier)
Baoyin, H., Li, J. F., & Gao, Y. F. 2002, Aerospace Science and Technology, 6, 295
Bauer, F. H., Bristow, J., Folta, D., et al., 1997, Proceedings of the AIAA GN&C Conference, August, 1997, New Orleans, USA, 657
Brouwer, D. 1959, AJ, 64, 378
Carter, T. E. 1990, Journal of Guidance Control Dynamics, 13, 183
Carter, T., & Humi, M. 1987, Journal of Guidance Control Dynamics, 10, 567
Clohessy, W. H., & Wiltshire, R. S. 1960, Journal of the Aerospace Sciences, 27, 653
Folta, D., Francesco, B. & Christopher, S. 1992, Proceedings of the 2nd AAS/AIAA Meeting, February, 1992, Colorado, USA, 803
Hou, X. Y., & Liu, L. 2011, MNRAS, 415, 3552
Inalhan, G., Tillerson, M., & How, J. P. 2002, Journal of Guidance, Control, and Dynamics, 25, 48
Kapila, V., Sparks, A. G., Buffington, J. M., & Yan, Q. 2000, Journal of Guidance, Control, and Dynamics, 23, 561
Kristiansen, R., & Nicklasson, P. J. 2009, Acta Astronautica, 65, 1537
Lawden, D. F. 1963, Optimal Trajectories for Space Navigation (London: Butterworths)
Liu, L., Hu, S. J., & Wang, X. 2006, An Introduction of Astrodynamics (Nanjing: Nanjing Univ. Press)
Melton, R. 2000, Journal of Guidance, Control, and Dynamics, 23, 604
Scharf, D. P., Hadaegh, F. Y., & Ploen, S. R. 2003, in 2003 American control conference, Denver, CO, June 4-6, 2003, 1733
Scharf, D. P., Hadaegh, F. Y., & Ploen, S. R. 2004, Journal of Guidance, Control, and Dynamics, 4, 2976
Schaub, H., & Alfriend, K. T. 1999, Flight Mechanics Symposium, NASA Goddard Space Flight Center, Greenbelt, MD, May 18-20, 1999, Paper No. 11
Schaub, H., Vadali, S. R., Junkins, J. L., & Alfriend, K. T. 2000, Journal of the Astronautical Sciences, 48, 69
Szebehely, V. 1967, Theory of orbits. The Restricted Problem of Three Bodies (New York: Academic Press)
Tillerson, M., & How, J. P. 2001, in Proceedings of the AIAA GN&C Conference, August, 2001, Montreal, Canada, Paper No. AIAA-2001-4092
Vadali, S. R., Vaddi, S. S., & Alfriend, K. T. 2002, International Journal of Robust and Nonlinear Control, 12, 97